R-branch heads was first suggested to W.T.R. by Michael Mumma (NASA/Goddard) in the context of the rocket-borne observations. We are also grateful for the assistance of Henry Murphy (PSI) with the experimental work and of Lauren Cowles, Margrethe DeFaccio, and Melanie Clawson (all of PSI) in the analysis of the data. This work was performed under Contract

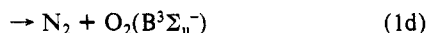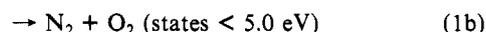# Product Branching Ratios from the $N_2(A^3\Sigma_u^+)$ + O_2 Interaction

Mark E. Fraser* and Lawrence G. Piper

Physical Sciences Inc., Research Park, P.O. Box 3100, Andover, Massachusetts 01810
(Received: November 13, 1987)

The product channels of the $N_2(A^3\Sigma_u^+,v=0-2)$ + O_2 interaction have been examined by using a discharge-flow apparatus. $N_2(A)$ was generated by energy transfer from Ar metastables and directly determined from Vegard–Kaplan emission. The branching ratios for N_2O and $O_2(B^3\Sigma_u^-)$ formation have been determined to be <0.2% and <15%, respectively. These results firmly establish quenching of $N_2(A^3\Sigma_u^+,v\leq2)$ by molecular oxygen to be a negligible source of atmospheric N_2O. The results for $O(^3P)$ production exceed the maximum possible branching ratio (two O atoms per $N_2(A)$) by a factor of 3. These results indicate that the Ar* + N_2 interaction produces N_2 metastable states, in addition to $N_2(A)$, capable of dissociating O_2.

Introduction

The product channels relevant to the $N_2(A^3\Sigma_u^+)$ + O_2 interaction are

$$N_2(A^3\Sigma_u^+) + O_2 \rightarrow N_2O + O \qquad (1a)$$

$$\rightarrow N_2 + O_2 \text{ (states < 5.0 eV)} \qquad (1b)$$

$$\rightarrow N_2 + O + O \qquad (1c)$$

$$\rightarrow N_2 + O_2(B^3\Sigma_u^-) \qquad (1d)$$

The aeronomic importance of an atmospheric N_2O source has led to several investigations of the branching ratio for N_2O formation from reaction 1a over the past several years.[1-6] These studies have differed significantly in the $N_2(A^3\Sigma_u^+)$ generation and determination techniques as well as the product analysis methods. As a result, a wide range of values have been reported. Those studies that have codischarged nitrogen/oxygen mixtures, a procedure that produces high concentrations of various nitrogen and oxygen excited electronic states as well as ground and metastable nitrogen and oxygen atoms, have produced the highest measurements of 60 ± 20%,[1] <10%,[2] and ~35%.[3] Iannuzzi et al.[4] were the first to examine this system using the cleaner metastable argon energy-transfer source of $N_2(A^3\Sigma_u^+)$. They reported a value of 2 ± 0.5% for the N_2O branching ratio. De-Souza et al.[5] determined a value of 1 ± 1% in a subsequent experiment that also used a metastable argon energy-transfer source. In light of the work of Iannuzzi et al.[4] and DeSouza et al.,[5] the N_2O branching ratio from reaction 1 requires only an accurate determination to finally resolve this issue.

Meyer et al.[7] demonstrated that one of the principal products of the interaction between $N_2(A)$ and O_2 is atomic oxygen, reaction 1c, in their observation of air afterglow emission when NO was added downstream in their discharge-flow reactor from their $N_2(A)/O_2$ interaction region. Iannuzzi et al.[4] estimated that approximately 65% of the $N_2(A)/O_2$ interactions lead to dissociation. This observation was based upon an indirect method of determining their $N_2(A)$ number density and so could be substantially in error. Golde and Moyle[8] examined the $N_2(A)/O_2$ interaction from the standpoint of examining vibrational effects on the products of various $N_2(A)$ reactions. They reported an enhanced efficiency for dissociation with vibrationally excited $N_2(A)$. They did not make absolute measurements, however. We have measured the atomic oxygen yield from the $N_2(A)$ + O_2 reaction using a direct determination of the $N_2(A)$ number density based upon absolute photometry and an absolute number density for the atomic oxygen product based upon resonance-fluorescence measurements in the vacuum ultraviolet.

Several groups have suggested that significant quenching of $N_2(A)$ by O_2 might result in excitation of $O_2(B^3\Sigma_u^-)$,[6,9,10] as shown in reaction 1d. This state is highly predissociative, so most of the excitation will result in O-atom production. A small fraction of the excitations, however, will give rise to fluorescence of the Schumann–Runge (SR) bands, $O_2(B^3\Sigma_u^- - X^3\Sigma_g^-)$. The principal Schumann–Runge bands emit in the ultraviolet between 250 and 400 nm, so that any emission from them should be interlaced with the Vegard–Kaplan and second-positive bands of nitrogen.

Experimental Section

This study used two separate but similar discharge-flow systems. The apparatus used for the $O(^3P)$ and $O_2(B^3\Sigma_u^-)$ studies is a 2-in. flow tube pumped by a Leybold–Heraeus Roots blower/forepump combination capable of producing linear velocities up to 5×10^3 cm s⁻¹ at a pressure of 1 Torr. The flow tube design is modular with separate source, reaction, and detection sections that clamp together with O-ring joints. The generation of $N_2(A^3\Sigma_u^+)$ in this apparatus has been previously described.[11] The detection region

(1) Zipf, E. C. *Nature (London)* **1980**, *287*, 523, 525.
(2) Black, G.; Hill, R. M.; Sharpless, R. L.; Slanger, T. G. *J. Photochem.* **1983**, *22*, 369.
(3) Zipf, E. C.; Prasad, S. S. *Nitrous Oxide Formation by Metastable $N_2(A^3\Sigma_u^+)$ Chemistry: A New Perspective on its Prospects*, preprint, 1984; includes reanalysis of Black (1983) data using $k = (1.5 \pm 0.15) \times 10^{-9}$ cm³ molecule⁻¹ s⁻¹ for the energy pooling reaction.
(4) Iannuzzi, M. P.; Jeffries, J. B.; Kaufman, F. *Chem. Phys. Lett.* **1982**, *87*, 570.
(5) DeSouza, A. R.; Touzeau, M.; Petitdidier, M. *Chem. Phys. Lett.* **1985**, *121*, 423.
(6) Eliasson, B.; Kogelschatz, U. *J. Chim. Phys. (Les Ulis, Fr.)* **1986**, *83*, 279.

(7) Meyer, J. A.; Setser, D. W.; Stedman, D. H. *J. Phys. Chem.* **1970**, *74*, 2238.
(8) Golde, M. F.; Moyle, A. M. *Chem. Phys. Lett.* **1985**, *117*, 375.
(9) Callear, A. B.; Wood, P. M. *Trans. Faraday Soc.* **1971**, *67*, 272.
(10) Dreyer, J. W.; Perner, D.; Roy, C. R. *J. Chem. Phys.* **1984**, *61*, 3164.
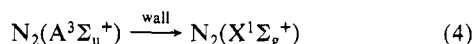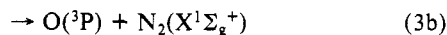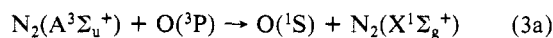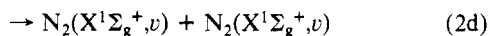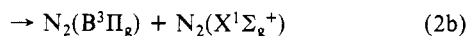
is a rectangular stainless-steel block bored out internally to a 2-in. circular cross section and coated with Teflon (Du Pont Poly TFE no. 852-201) to retard surface recombination of atoms. Use of a black primer prior to the Teflon coating reduces scattered light inside the block dramatically. The block has two sets of viewing positions consisting of four circular ports each on the four faces of the block. These circular ports accommodate vacuum-ultraviolet resonance lamps, vacuum UV and visible monochromator interfaces, laser delivery sidearms, a photometer consisting of a lens and several baffles to restrict the field of view to the center of the reactor, and a photomultiplier/interference filter combination to detect light in a restricted wavelength region.

The N_2O study used a similar 5-cm diameter, 50-cm-long quartz flow tube equipped with a Pyrex trap. The total flow rate was typically 1.9 mmol s^{-1} at a pressure of 2.6 Torr. The input O_2, N_2, and Ar gases were purified by flowing them through cryogenic traps of 5-Å molecular sieve prior to their entry into the reactor. The trap on the nitrogen gas line was immersed in liquid nitrogen, while those for argon and oxygen were maintained at −95 °C with methanol/liquid N_2 slush baths. The argon was further purified with a commercial scrubber that claims to reduce O_2 and H_2O impurities to ≤0.1 ppm volume. With this purification scheme CO_2 remained as the only detected impurity (due to outgassing of the flow tube walls).

Both experimental systems used a hollow-cathode discharge source of conventional design[12] operating at 240 V dc and 3 mA to produce argon metastables. The reaction between metastable Ar($^3P_{0,2}$) and molecular nitrogen excites $N_2(C^3\Pi_u)$,[13] which quickly cascades radiatively to the metastable $A^3\Sigma_u^+$ state via the $B^3\Pi_g$ state.

Results

Kinetics. In addition to reactions 1a–d, the reactions relevant to $N_2(A)$ loss in the flow tube are

$$N_2(A^3\Sigma_u^+) + N_2(A^3\Sigma_u^+) \rightarrow N_2(C^3\Pi_u) + N_2(X^1\Sigma_g^+) \quad (2a)$$

$$\rightarrow N_2(B^3\Pi_g) + N_2(X^1\Sigma_g^+) \quad (2b)$$

$$\rightarrow N_2(X^1\Sigma_g^+) + N_2(\text{Herman IR}) \quad (2c)$$

$$\rightarrow N_2(X^1\Sigma_g^+,v) + N_2(X^1\Sigma_g^+,v) \quad (2d)$$

$$N_2(A^3\Sigma_u^+) + O(^3P) \rightarrow O(^1S) + N_2(X^1\Sigma_g^+) \quad (3a)$$

$$\rightarrow O(^3P) + N_2(X^1\Sigma_g^+) \quad (3b)$$

$$N_2(A^3\Sigma_u^+) \xrightarrow{\text{wall}} N_2(X^1\Sigma_g^+) \quad (4)$$

Reported rate constants for the energy-pooling reactions[14,15] range from 1×10^{-10} to 1.4×10^{-9} cm^3 molecule^{-1} s^{-1}. At the $N_2(A)$ number densities encountered in these experiments, energy-pooling losses are calculated to have an effective first-order loss rate of ≪20 s^{-1}. The rate coefficient for reaction 3 has been measured by Piper et al.[16] as 3×10^{-11} cm^3 molecule^{-1} s^{-1}. At the highest O-atom number densities expected for these experiments, i.e., unit dissociation of O_2 by $N_2(A)$, the first-order rate is <1 s^{-1}. The loss of $N_2(A)$ on the walls is diffusion controlled and has a rate coefficient of about 30 s^{-1} at 2.6 Torr in a 5-cm diameter tube. The radiative decay of $N_2(A)$ is also slow, 1.9 s^{-1}.[17]

For these experiments excess oxygen concentrations have been used, typically >10^{15} molecules cm^{-3}. The rate coefficient for the

(11) Piper, L. G.; Cowles, L. M.; Rawlins, W. T. *J. Chem. Phys.* **1986,** *85,* 3369.

(12) Stedman, D. H.; Setser, D. W. *Prog. React. Kinet.* **1971,** *6,* 193; *Chem. Phys. Lett.* **1971,** *2,* 193.

(13) Sadeghi, N.; Setser, D. W. *Chem. Phys. Lett.* **1981,** *82,* 44.

(14) Hays, G. N.; Oskam, H. J. *J. Chem. Phys.* **1973,** *59,* 1507.

(15) Hill, R. M.; Gutcheck, R. A.; Huestis, D. L; Mukherjee, K.; Lorents, D. C. *Studies of E-beam Pumped Molecular Lasers*; SRI Report No. MP74-39 under ARPA Contract N. N00014-72-C-0478 (1974).

(16) Piper, L. G.; Caledonia, G. E.; Kennealy, J. P. *J. Chem. Phys.* **1981,** *75,* 2847.

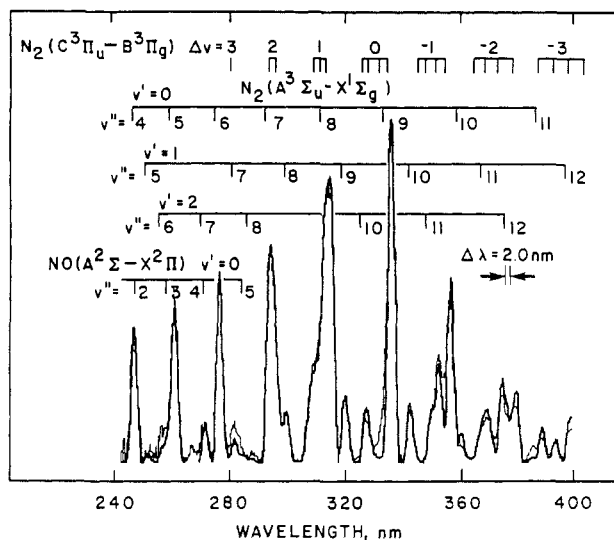(17) Shemansky, D. E. *J. Chem. Phys.* **1969,** *51,* 689.

Figure 1. Data (light line) and best fit (dark line) to Vegard–Kaplan emission at 2.6 Torr. Included in the fit are first-positive emission, NO γ bands, and OH A–X emission (not shown) at 307 nm. The spectroscopic data have been obtained from the literature.[17,23,24]

deactivation of $N_2(A)$ by O_2 increases with vibrational level[18] and has a value of 2.3×10^{-12} cm^3 molecules^{-1} s^{-1} for $v = 0$. The first-order deactivation rate coefficient at these oxygen concentrations is >2000 s^{-1}. Thus, the $N_2(A)$ losses from reactions 2–4 can be neglected compared to losses via reaction 1. There are no loss processes for O and N_2O during the relatively short flow time between O_2 introduction and product detection or collection. In terms of the flow rates of the gases we have

$$f_{N_2O} = (k_{1a}/k_1)f_{N_2(A)} \quad (5a)$$

$$f_O = (2k_{1c}/k_1)f_{N_2(A)} \quad (5b)$$

The flow rate of $N_2(A)$ through the interaction region is given by its number density in the interaction region times the volumetric flow rate in the reactor:

$$f_{N_2(A)} = [N_2(A)]A\bar{v} \quad (6)$$

where A is the reactor cross sectional area and $\bar{v}$ is the bulk flow velocity. All three terms of eq 6 have radial dependence:[19]

$$dA(r) = 2\pi r \, dr$$

$$[N_2(A)](r) = [N_2(A)]_0 J_0(\lambda r/a)$$

$$v(r) = 2\bar{v}\{1 - (r/a)^2\}$$

where $[N_2(A)]_0$ is the $N_2(A)$ number density along the flow tube axis (the center-line number density), a is the flow tube radius, J_0 is the zero-order Bessel function, and λ is its first root (2.405). The integral expression for eq 6 becomes

$$f_{N_2(A)} = 4\pi a^2 [N_2(A)]_0 \bar{v} \int_0^1 J_0(\lambda s)(1 - s^2)s \, ds \quad (7)$$

with $s = r/a$. Simple numerical integration gives

$$f_{N_2(A)} = 0.60[N_2(A)]_0 A\bar{v} \quad (8)$$

We have shown elsewhere[20] that the average $N_2(A)$ number density that we observe by looking across the flow tube is related to the center-line number density by

$$[N_2(A)] = 0.601[N_2(A)]_0 \quad (9)$$

Thus, the corrections for radial density and velocity gradients cancel, and we obtain the expression shown in eq 6.

N_2O Formation. Vegard–Kaplan spectra were taken with a 1.26-m Spex monochromator equipped with a grating blazed at

(18) Piper, L. G.; Caledonia, G. E.; Kennealy, J. P. *J. Chem. Phys.* **1981,** *74,* 2888.

(19) Ferguson, E. E.; Fehsenfeld, F. C.; Schmeltekopf, A. L. *Adv. At. Mol. Phys.* **1970,** *5,* 1.

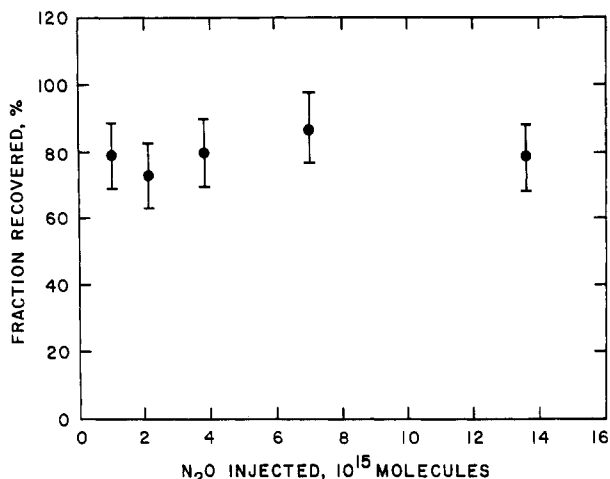(20) Piper, L. G. *J. Chem. Phys.* **1988,** *88,* 231.

Figure 2. N_2O trapping efficiency. The data are presented as the fraction of N_2O recovered, in percent, versus the mass of N_2O injected.

500 nm and operated in first order at a spectral resolution of 2 nm. The relative response of the spectrometer was determined with a deuterium lamp and the absolute response with the O + NO chemiluminescent reaction.[21] A computer-controlled data acquisition system collected the spectra. The absolute $N_2(A,v)$ number densities were determined by using a spectral-generation linear least-squares fitting technique.[22] The spectroscopic data are from Lofthus and Krupenie[23] and Huber and Herzberg.[24] The Einstein coefficients for the $N_2(A-X)$ transitions are from Shemansky.[17] He estimated them to carry a 20% uncertainty. Previous experiments on the energy transfer between $N_2(A)$ and NO,[11] however, indicated that Shemansky's transition probabilities are likely to be 20%–40% too large. We have chosen not to revise the $N_2(A-X)$ transition probabilities until this issue has been resolved definitively.

Figure 1 shows a typical data set and best fit. The other band systems typically encountered with Vegard–Kapaln emission have also been incorporated into the fit. The $N_2(A)$ number densities were typically 3.5×10^9, 1.7×10^9, and 8×10^8 molecules cm^{-3}, respectively, for $v = 0-2$. Although not determined directly, an upper limit of $\leqslant 3 \times 10^8$ molecules cm^{-3} may be set for $v = 3$.

Owing to the low $N_2(A)$ number densities generated by the energy-transfer source, the N_2O product yields are low and could be dominated by impurities. Accurate N_2O detection is therefore the key to determining the branching ratio. Previous studies have detected N_2O by mass spectrometry,[1,5] gas chromatography with electron-capture detection,[2,4] and infrared absorption.[6] The mass spectrometer detection technique used by Zipf[1] and DeSouza et al.[5] encountered difficulties because they did not employ chromatography to separate NO from N_2O and so were unable to monitor the fragment ion at mass 30. The parent ion at mass 44 was therefore monitored despite the coincidence of CO_2.

The N_2O analysis technique chosen for this study was gas chromatography with mass spectrometric detection (GCMS). We have employed a chromatographic column capable of resolving NO from N_2O so mass 30 could be used to determine N_2O unambiguously. The column was 5 ft × $^1/_8$-in. o.d. Carbosieve S-II, similar to that used by Iannuzzi et al.[4] N_2O from the $N_2(A)$ + O_2 interaction was collected in a Pyrex trap immersed in liquid nitrogen followed by GCMS analysis of the trap contents. Typical trapping times were 2 h.

The GCMS was calibrated with standards generated by static dilution of cylinder N_2O. Calibration was performed by introducing low pressures of the standards into a U-trap followed by
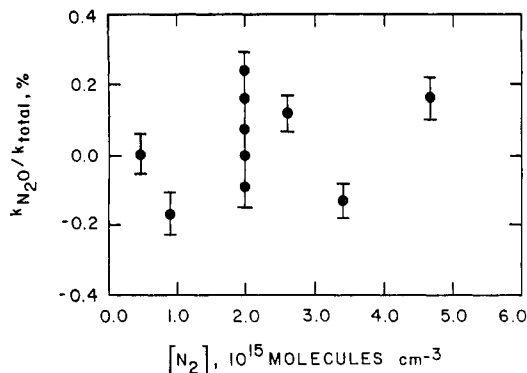

Figure 3. Results for the N_2O branching ratio.

TABLE I: Values of k_{N_2O}/k_{total} from $N_2(A^3\Sigma_u^+)$ + O_2

investigator	determined k_{N_2O}/k_{total}, %
Zipf (1980)[1]	60 ± 20
Iannuzzi et al. (1982)[4]	2 ± 0.5
Black et al. (1983)[2]	<10
Zipf (1984)[3] reanalysis of Black et al.[2]	40 ± 15
DeSouza et al. (1985)[5]	1 ± 1
Eliasson (1986)[6]	4
this work (1988)	<0.2

injection into the GCMS. The calibration curve was linear over the N_2O mass range encountered in these studies with a detection limit of 10 ng (1.4×10^{14} molecules).

The N_2O trapping efficiency was determined by injecting a small volume of the calibration mixture into the flow reactor at the flow rate and pressure of normal operation. Figure 2 shows that the trapping efficiency was 80 ± 5% over the entire mass range of interest.

The total number of N_2O molecules, N_{N_2O}, produced from the $N_2(A)$ + O_2 interaction is equal to the total time integrated flow past the observation point. From eq 5a and 6 we have

$$N_{N_2O} = f_{N_2O}\Delta t \tag{10}$$

$$N_{N_2O} = (k_{1a}/k_1)[N_2(A)]A\bar{v}\Delta t \tag{11}$$

Although no N_2O was observed in the input gases or argon with the discharge on, measurable levels were detected from discharged argon with added nitrogen. Therefore, the data were taken in pairs with runs of added oxygen contrasted with runs without added oxygen. In all, 10 data points were obtained at nitrogen concentrations of 4.5×10^{14}–4.64×10^{15} molecules cm^{-3}. The entire data set is shown in Figure 3. The N_2O yields have been corrected for background and trapping efficiency. The $N_2(A)$ concentrations were relatively invariant over the entire nitrogen concentration range. The determined N_2O branching ratios exhibit no dependence on $[N_2]$. The recommended value for the N_2O branching ratio that corresponds to the 90% confidence level is k_{1a}/k_1 <0.2%. Table I shows a comparison of this result with previous data. The value for the N_2O branching ratio determined here is significantly lower than the results of Zipf.[1,3] Considering the large value initially claimed for this reaction, the difference between this result and those of Iannuzzi et al.[4] and DeSouza et al.[5] is small.

If we assume an upper limit of k_{1a}/k_1 of 0.2% and that the branching ratio is zero for vibrational levels $v = 0, 1$, an upper limit of $\leqslant 1.5$% is calculated for $v = 2$. This value is negligibly small and indicates that if there is a dramatic branching ratio increase with increasing vibrational excitation, as has been recently suggested,[25] it must occur for vibrational levels $v \gg 2$.

$O(^3P)$ Formation. In these experiments, large flows of molecular oxygen are added to our flow reactor just upstream from the point at which the $N_2(A)$ number density is determined. This essentially quenches all of the $N_2(A)$ in a distance sufficiently

(21) Fontijn, A.; Meyer, C. B.; Schiff, H. I. *J. Chem. Phys.* **1964**, *40*, 64.
(22) Fraser, M. E.; Rawlins, W. T.; Miller, S. M. *J. Chem. Phys.* **1988**, *88*, 538.
(23) Lofthus, A.; Krupenie, P. H. *J. Phys. Chem. Ref. Data* **1977**, *6*, 113.
(24) Huber, K. P.; Herzberg, G. *Molecular Spectra and Molecular Structure IV. Constants of Diatomic Molecules*; Van Nostrand Reinhold: New York, 1979.

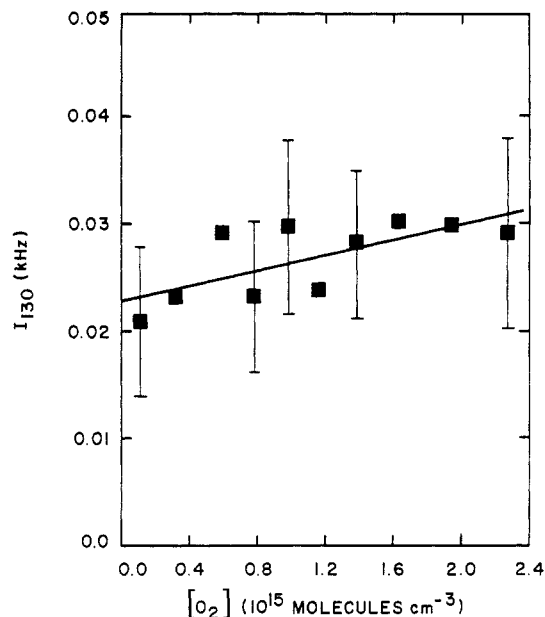(25) Zipf, E. C., private communication, 1987.

Figure 4. Atomic oxygen resonance fluorescence signal produced in the reaction between $N_2(A)$ and O_2.

TABLE II: $O(^3P)$ Produced upon Adding O_2 to a Flow of $N_2(A)$[a]

trial	$10^{-9}[N_2(A)]$, molecules cm^{-3}	$\% v > 0$	$10^{-10}[O]$, atoms cm^{-3}	$[O]/[N_2(A)]$
1	1.4 ± 0.4	46	1.3 ± 0.2	9.2 ± 3.1
2	2.1 ± 0.6	8	1.1 ± 0.2	5.2 ± 1.7
3	3.0 ± 0.9	0	1.9 ± 0.3	6.2 ± 2.1
4	3.3 ± 1.0	50	2.5 ± 0.4	7.7 ± 2.6
5	2.4 ± 0.7	49	1.5 ± 0.2	6.3 ± 2.1
6	2.4 ± 0.7	36	1.5 ± 0.2	6.3 ± 2.1
7	2.3 ± 0.7	19	1.4 ± 0.2	6.1 ± 2.0
8	2.3 ± 0.7	7	1.4 ± 0.2	5.8 ± 1.9
				av 6.6 ± 1.3

[a] The third column indicates the percent of the $N_2(A)$ population in vibrational levels greater than zero. The average value at bottom is shown with 1 standard deviation error.

short that diffusive losses of the $N_2(A)$ can be neglected, and all losses of $N_2(A)$ result, therefore, from its interaction with O_2. At some point downstream, the atomic oxygen produced is determined by atomic resonance fluorescence at 130.4 nm. From eq 5b the reaction branching ratio is

$$\frac{k_{1c}}{k_1} = \frac{f_O}{2N_2(A)} = \frac{[O]}{2[N_2(A)]} \qquad (12)$$

Absolute atomic oxygen atom number densities have been determined by resonance fluorescence measurements in the vacuum ultraviolet. We have previously described our apparatus configuration and procedures for vacuum UV resonance fluorescence in some detail.[26,27] In these measurements, the resonance fluorescence was calibrated by the well-known NO titration of atomic nitrogen:

$$N + NO \rightarrow N_2 + O \qquad (13)$$

In excess atomic nitrogen, the atomic oxygen produced in reaction 13 is identically equal to the amount of nitric oxide added to the reactor.

The resonance-fluorescence lamp produces some atomic oxygen by O_2 photolysis in addition to that created by $N_2(A)$ dissociation of molecular oxygen. To correct for this, we measured the atomic oxygen resonance-fluorescence signal as a function of molecular oxygen addition and then extrapolated the results to zero molecular oxygen addition. Provided that the initial molecular oxygen number density is sufficient to quench all of the $N_2(A)$ in a short reaction distance, this procedure is adequate for the experiment. In reality, of course, at very low molecular oxygen number densities, the resonance-fluorescence signal goes to zero as the O_2 number density approaches zero. To check that the resonance-fluorescence signal was not significantly attenuated by the large additions of O_2, we looked at the attenuation of the 130.4-nm line produced in a discharge lamp as a functon of O_2 number density. This experiment showed that the 130.4-nm radiation was attenuated by less than 1% for $[O_2] < 3 \times 10^{15}$ molecules cm^{-3}. The bulk of our observations were at O_2 number densities below 2×10^{15} molecules cm^{-3}.

Figure 4 shows the resonance fluorescence signal as a function of O_2 addition in the presence of $N_2(A)$. The intercept of the best-fit straight line through the data gives the atomic oxygen number density produced from the dissociation of molecular oxygen by $N_2(A)$. We made several measurements for different $N_2(A)$ number densities and for different levels of vibrational excitation of the $N_2(A)$. Table II summarizes our results. We are hard pressed to find explanations for the excess of O produced over that which would be expected were the branching ratio, k_{1c}/k_1, to be unity. Part of the discrepancy could be accounted for by uncertainty (20%–40%) in the $N_2(A)$ Einstein coefficients.[11] This accounts only for a small part of the difference, however. We checked our atomic oxygen calibration by measuring the atomic oxygen formed in the slow reaction between $N(^4S)$ and O_2. These experiments followed the production of atomic oxygen as a function of $[O_2]$ for known N-atom number densities and reaction times and gave a rate coefficient for this reaction in excellent agreement with the values in the literature derived from monitoring N-atom decays.[28] The implication of the measurements, therefore, is that our $N_2(A)$ number density determination is badly in error or else that some unknown energy carrier, sufficiently energetic to dissociate molecular oxygen, accompanies the $N_2(A)$ down the flow tube. We believe that our absolute photometry measurements are reasonably accurate ($\pm 30\%$). Our determinations of the formation of $N_2(C)$ and the Herman infrared system in $N_2(A)$ energy pooling agree well with other reports in the literature.[20] These measurements also depend upon absolute photometry to determine $N_2(A)$ number densities. We therefore conclude that the $N_2(A)$ number density determination has been performed correctly. We observed similar discrepancies between [O] produced and $[N_2(A)]$ in the reactor several years ago when the O/NO air afterglow was used as the O-atom monitor. That apparatus was somewhat different from the current one, and calibration procedures have improved. The result is unchanged, however.

The possibility certainly exists that the energy transfer between $Ar^*(^3P_{0,2})$ and N_2 does produce some metastable nitrogen species in addition to $N_2(A)$. The extremely good correlation between the rate coefficients for quenching Ar^* by N_2 and for exciting $N_2(C^3\Pi_u)$ in the $Ar^* + N_2$ reaction demonstrates clearly that $N_2(C)$ is the principal product of the Ar^*/N_2 interaction.[13] The $N_2(C)$ is converted to $N_2(A)$ in a radiative cascade via $N_2(B^3\Pi_g)$. The B-state is sufficiently long lived that it experiences many collisions before it radiates. Indeed, at pressures on the order of a few Torr with N_2 mole fractions of a few percent, the principal deactivation mechanism for the $N_2(B)$ may be quenching rather than radiation. While quenching of $N_2(B)$ has always been assumed to end up in the A-state, this assumption has never been tested experimentally. What is needed are simultaneous determinations of metastable argon number densities via resonance absorption in the near infrared and absolute photometric measurements of the Vegard–Kaplan bands to determine $N_2(A)$ number densities. Typically, metastable argon number densities tend to be on the order[29] of 2×10^{10} atoms cm^{-3}, while those of

(26) Rawlins, W. T.; Piper, L. G. *Proc. Soc. Photo-Opt. Instrum. Eng.* **1981**, *279*, 58.

(27) Piper, L. G.; Donahue, M. E.; Rawlins, W. T. *J. Phys. Chem.* **1987**, *91*, 3883.

(28) Becker, K. H.; Groth, W.; Kley, D. *Z. Naturforsch, A: Phys., Phys. Chem., Kosmophys.* **1969**, *24*, 1280.
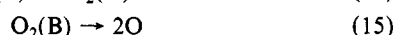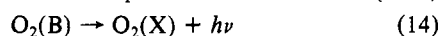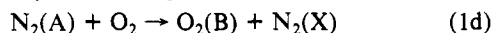
(29) Piper, L. G.; Velazco, J. E.; Setser, D. W. *J. Chem. Phys.* **1973**, *59*, 3323.

$N_2(A)$ tend more to be in the 10^9 molecules cm^{-3} range.[20] To our knowledge, however, no one has ever made simultaneous measurements. Dreiling and Setser,[30] in studies on the excitation of mercuric halides by $N_2(A)$, also saw some evidence for the formation of another nitrogen metastable in addition to $N_2(A)$. They were unable to identify this other state. Their observations indicated, however, that its internal energy was in excess of 6.5 eV, more than enough to dissociate O_2.

If the energy-transfer reaction between $Ar^*(^3P_{0,2})$ and N_2 does indeed form a metastable nitrogen state in addition to $N_2(A^3\Sigma_u^+)$, then Iannuzzi et al.'s[4] estimate of 65%–80% of $N_2(A) + O_2$ collisions leading to oxygen dissociation is uncertain. What they demonstrated is that 65%–80% of the metastable nitrogen molecules produced in the $Ar^* + N_2$ interaction dissociate molecular oxygen. Our results indicate that most of these metastable nitrogen molecules are *not* $N_2(A^3\Sigma_u^+)$. Thus the actual dissociation yield is still unsettled. Conceivably, no dissociation results from the $N_2(A) + O_2$ interaction; all observed dissociation could have been effected by the companion nitrogen metastable. The results for O_2 dissociation in no way detract from the validity of our measurements on N_2O formation. N_2O clearly is not a product of the $N_2(A) + O_2$ reaction or of the reaction of the companion nitrogen metastable with molecular oxygen.

$O_2(B^3\Sigma_u^-)$ *Formation.* We looked for Schumann–Runge emission when sufficient molecular oxygen was added to our reactor to quench out approximately half of the $N_2(A)$. These experiments were done in the presence of CH_4 so that only $N_2(A,v'=0)^{31,32}$ was in the reactor. In this case, only $O_2(B,v'=0)$ is energetically available as an energy acceptor. We failed to observe any changes in the relative spectrum indicating that Schumann–Runge emission was not significant. We can use this null result to set an upper limit on the channel of O_2 quenching of $N_2(A)$ which produces $O_2(B)$.

Our kinetic analysis is based upon the following reaction scheme:

$$N_2(A) + O_2 \rightarrow O_2(B) + N_2(X) \qquad (1d)$$

$$\rightarrow \text{other products} \qquad (1a\text{-}c)$$

$$O_2(B) \rightarrow O_2(X) + h\nu \qquad (14)$$

$$O_2(B) \rightarrow 2O \qquad (15)$$

The rate equation describing the rate of change in the number density of $O_2(B)$ with time is

$$d[O_2(B)]/dt = k_{1d}[O_2][N_2(A)] - (k_{14} + k_{15})[O_2(B)] \qquad (16)$$

Because the predissociative lifetime for $O_2(B,v'=0)$ is only 53 ps,[33] the $O_2(B)$ is in steady state in the detector's field of view. Thus setting eq 16 to zero and rearranging give

$$I_{O_2(B)} = k_{14}[O_2(B)] = k_{1d}[O_2][N_2(A)]/(1 + k_{15}/k_{14}) \qquad (17)$$

We can use the fact that the $N_2(A)$ number density is given by the intensity of the Vegard–Kaplan emission divided by the Einstein coefficient along with eq 17 to derive an expression that gives the branching ratio, k_{1d}/k_1 in terms of observed intensities:

$$\frac{k_{1d}}{k_1} = \frac{I_{O_2(B)}A_{N_2(A)}(1 + k_{15}/k_{14})}{I_{N_2(A)}[O_2]} \qquad (18)$$

In this form, only relative band intensities matter and system calibrations converting observed intensities into absolute photon-emission rates are unnecessary.

The strongest Schumann–Runge band which suffers least from overlap with the Vegard-Kaplan bands is the 0,13 transition at 323.4 nm: 15% of the emission from $O_2(B,v'=0)$ appears in this band.[34] For comparison, approximately 4% of the emission from $N_2(A,v'=0)$ appears in the 0,10 band at 360.3 nm.[17] Figure 5
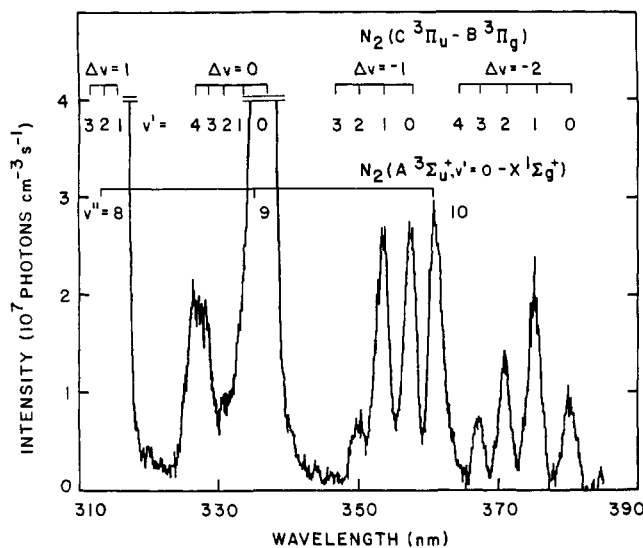

Figure 5. Vegard–Kaplan and second-positive bands (formed from N_2-(A) energy pooling) in the presence of 3.5 mTorr of molecular oxygen.

shows the spectrum of the Vegard–Kaplan and second-positive bands of nitrogen in the presence of 1.13×10^{14} molecules cm^{-3} of molecular oxygen. Clearly, a band at 323 nm with one-fifth the intensity of the 0,10 Vegard–Kaplan band ought to be apparent. None is. Given that the total rate coefficient for quenching $N_2(A,v'=0)$ by O_2 is 2.3×10^{-12} cm^3 $molecule^{-1}$ s^{-1},[18] and that the $N_2(A)$ Einstein coefficient is 0.5 s^{-1}, we infer that less than 15% of the energy-transfer events between $N_2(A,v'=0)$ and O_2 result in excitation into the $O_2(B)$ state. Similar observations in the absence of CH_4 also failed to reveal any emissions that could be attributed to $O_2(B)$ fluorescence. We conclude, therefore, that $N_2(A,v'=1,2)$ also does not excite Schumann–Runge emission. As was the case for the N_2O study, the possible presence of a metastable nitrogen species in addition to $N_2(A)$ does not affect this conclusion. Neither $N_2(A)$ *nor* its companion metastable excite the $O_2(B)$ state.

Conclusions

From the results of this study and those of Iannuzzi et al.[4] and DeSouza et al.,[5] the reaction $N_2(A^3\Sigma_u^+,v\leqslant2) + O_2$ can no longer be considered as a source of nitrous oxide in the upper atmosphere unless higher $(v \gg 2)$ vibrational levels are involved. Similarly, this reaction cannot account for nitrous oxide formation in discharged oxygen/nitrogen mixtures nor from lightning. Although production of N_2O by discharges and lightning is well documented,[35-37] the nitrous oxide formation mechanism(s) are not yet fully understood.

Schumann–Runge emission has not been observed from the $N_2(A) + O_2$ interaction which places a bound of <15% on the branching ratio for $O_2(B^3\Sigma_u^-)$ formation. Thus, the preferred reaction channels must be reactions 1b and/or 1c. We have attempted to measure the branching ratio for $O(^3P)$ formation directly by simultaneous determination of $[N_2(A)]$ from Vegard–Kaplan photoemission rates and $[O(^3P)]$ by UV resonance fluorescence. The results indicate a branching ratio fraction of 6.6 ± 1.3, which is a factor of 3 in excess of the maximum value of 2. These results indicate that the $Ar^* + N_2$ interaction produces N_2 states, in addition to $N_2(A)$, that are capable of dissociating O_2.

(30) Dreiling, T. D.; Setser, D. W. *Chem. Phys. Lett.* **1980**, *74*, 211.
(31) Piper, L. G.; Marinelli, W. J.; Rawlins, W. T.; Green, B. D. *J. Chem. Phys.* **1985**, *83*, 5602.
(32) Thomas, J. M.; Jeffries, J. B.; Kaufman, F. *Chem. Phys. Lett.* **1983**, *102*, 50.
(33) Lewis, B. R.; Berzins, L.; Carver, J. H.; Gibson, S. T. *J. Quantum Spectrosc. Radiat. Transfer* **1986**, *36*, 187.
(34) Allison, A. C.; Dalgarno, A.; Pasachoff, N. W. *Planet. Space Sci.* **1971**, *19*, 1463.
(35) Hill, R. D.; Linker, R. G.; Coucouvinos, A. *J. Geophys. Res.* **1984**, *89*, 1411.
(36) Donohoe, K. G.; Shair, F. H.; Wulf, O. R. *Ind. Eng. Chem. Fundam.* **1977**, *16*, 208.
(37) Levine, J. S.; Shaw, E. F. *Nature (London)* **1983**, *303*, 312.